

Supplementary Information

Structure-property relationship of homochiral and achiral supramolecular isomers in one-pot synthesis

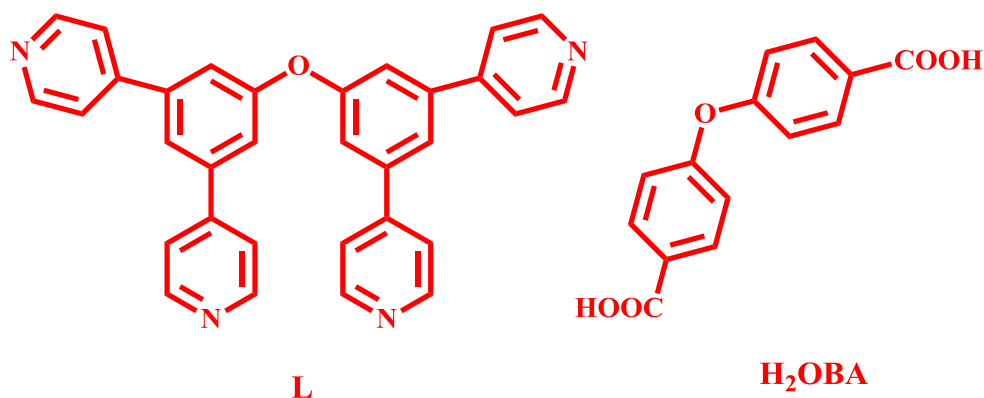
Ling Qin, Jin-Song Hu, Ming-Dao Zhang, Zi-Jian Guo, He-Gen Zheng

Contents

1. Experimental Section.
2. Scheme 1. Diarboxylate H₂OBA and N-containing L ligand.
3. Crystal data for compounds **1** and **2**.
4. Fig. S1 Powder X-ray diffraction patterns of complex **1**.
5. Fig. S2 Powder X-ray diffraction patterns of complex **2**.
6. Fig. S3. Additional figures for **1**.
7. Fig. S4. The solid-state CD spectra of bulk samples of **1**.
8. Fig. S5. An electric hysteresis loop of MOF **1** at the temperature of liquid nitrogen.
9. Fig. S6. Additional figures for **2**.
10. Fig. S7 Frequency dependence of the in-phase and out-of-phase ac susceptibility of **2**.
11. Fig. S8. IR spectra of complex **1**.
12. Fig. S9. IR spectra of complex **2**.
13. Fig. S10. UV-vis absorbance spectra of compounds **1** and **2** at room temperature.
14. Fig. S11. Variable temperature PXRD spectra of MOF **1**.
15. Fig. S12. The TGA diagrams of complexes **1** and **2**.
16. Table S1. Selected Bond Lengths (Å) and Angles (deg) for Complexes **1** and **2**.

1. Experimental Section.

Materials and Measurements. Reagents and solvents employed were commercially available. L ligand was prepared on the basis of palladium-catalyzed cross-coupling reactions.¹ IR absorption spectra of the compounds **1** and **2** were recorded in the range of 400–4000 cm⁻¹ on a Nicolet (Impact 410) spectrometer with KBr pellets (5 mg of sample in 500 mg of KBr). C, H and N analyses were carried out with a Perkin Elmer 240C elemental analyzer. Powder X-ray diffraction (PXRD) measurements were performed on a Bruker D8 Advance X-ray diffractometer using Mo-K_α radiation ($\lambda = 0.71073 \text{ \AA}$), in which the X-ray tube was operated at 40 kV and 40 mA. The as-synthesized samples were characterized by thermogravimetric analysis (TGA) on a Perkin Elmer thermogravimetric analyzer Pyris 1 TGA up to 1023 K using a heating rate of 10 K min⁻¹ under N₂ atmosphere. The second-order nonlinear optical intensity was estimated by measuring a powder sample relative to urea. A pulsed Q-switched Nd:YAG laser at a wavelength of 1064 nm was used to generate a SHG signal. The backscattered SHG light was collected by a spherical concave mirror and passed through a filter that transmits only 532 nm radiation. The circular dichroism (CD) spectra of **1** were recorded at room temperature with a Jasco J-810(S) spectropolarimeter (KBr pellets). The electric hysteresis loops were recorded on a Ferroelectric Tester Precision Premier II made by Radiant Technologies, Inc. Direct current (DC) magnetic susceptibility and magnetization measurements were carried out on a Quantum Design MPMS-XL7 superconducting quantum interference device (SQUID) magnetometer. The alternating current (AC) susceptibility down to 1.8 K was performed in a zero DC field and a 5.0 Oe field oscillating at frequencies in the 1–1500 Hz range. The gas sorption isotherms were measured by Micromeritics ASAP 2020 M+C surface area analyzer.



Scheme 1. Diarboxylate and N-containing L ligand.

Synthesis of complexes 1 and 2: A mixture of H₂O/DMF/CH₃CN containing the L (47.8 mg, 1 mmol), H₂OBA (25.8 mg, 1 mmol) and Co(NO₃)₂·6H₂O (58.2 mg, 2 mmol) were mixed in a Teflon vessel within the autoclave. The vessel was heated at 95 °C for 72 h and then cooled to room temperature. The purple (**1**) and red crystals (**2**) were obtained. Yields of the reaction were ca. 50% and 35% based on L ligand, respectively. Elemental analysis calcd. for CoC₄₆H₃₂N₄O₇ (**1**): C, 68.07; H, 3.97; N, 6.90, Found: C, 68.04; H, 3.92; N, 6.58. Calcd. for Co₅C₁₂₇H₁₁₇N₁₅O₂₆ (**2**): C, 59.49; H, 4.60; N, 8.19, Found: C, 60.04; H, 4.20; N, 8.31. The IR spectra of the corresponding complexes are shown in the Figs. S8-S9.

X-ray Crystallography. Crystallographic data of **1** and **2** were collected on a Bruker Apex Smart CCD diffractometer with graphite-monochromated Mo K α radiation ($\lambda = 0.71073$ Å) using the ω -scan technique. The intensity data were integrated by using the SAINT program.² An empirical absorption correction was applied using the SADABS program.³ The structures were solved by direct method and the nonhydrogen atoms were located from the trial structures and then refined anisotropically with SHELXTL using full-matrix least-squares procedures based on F² values. The positions of the non-hydrogen atoms were refined with anisotropic displacement factors. The hydrogen atoms were positioned geometrically by using a riding model. The distribution of peaks in the channels of **2** was chemically featureless to refine, using conventional discrete-atom models. To resolve these issues,

the contribution of the electron density by the remaining solvent molecules was removed by the SQUEEZE routine in PLATON.⁴ The number of electrons thus located, 804 per unit cell, is included in the formula, formula weight, calculated density, μ and $F(000)$. This residual electron density was assigned to five of the DMF molecules, [804 /4 = 201e per two ligands].

Crystal data: for **1**: [C₄₆H₃₂CoN₄O₇], $M_r = 811.69$, hexagonal, space group $P6_5$, $a = 13.5091(7)$, $b = 13.5091(7)$, $c = 36.8157(19)$ Å, $\gamma = 120.00$, $V = 5818.6(5)$ Å³, $Z = 6$, $D_c = 1.390$ g·cm⁻³, $\mu(\text{Mo-K}\alpha) = 0.502$ mm⁻¹, $T = 296(2)$ K, 33619 reflections measured, 7694 independent reflections ($R_{\text{int}} = 0.0865$), final $R_1 [I > 2\sigma(I)] = 0.0309$ and final $wR(F_2) = 0.0567$. Further, refinement in the chiral space group $P6_5$ assigns a reasonable absolute structure parameter (the Flack parameter = $-0.003(7)$). For **2**: [C₁₂₇H₁₁₇Co₅N₁₅O₂₆], $M_r = 2564.04$, monoclinic, space group $C2/c$, $a = 27.4499(17)$, $b = 17.0811(10)$, $c = 29.4964(18)$, $\beta = 108.5660(10)$, $V = 13110.4(14)$ Å³, $Z = 4$, $D_c = 1.299$ g·cm⁻³, $\mu(\text{Mo-K}\alpha) = 0.693$ mm⁻¹, $T = 296(2)$ K, 58499 reflections measured, 14987 independent reflections ($R_{\text{int}} = 0.0619$), final $R_1 [I > 2\sigma(I)] = 0.0426$ and final $wR(F_2) = 0.1125$.

Gas Sorption Measurements

In the gas sorption measurement, Ultra-high-purity grade, N₂, H₂, CO₂ and CH₄ (>99.999%) were used throughout the adsorption experiments. All of the measured sorption isotherms have been repeated several times to confirm the reproducibility within experimental error. Adsorption measurements (up to 1 bar) were performed on Micromeritics ASAP 2020 M+C surface area analyzer. About 110 mg of samples **2** were activated at 80 °C for 10 hours by using the “outgas” function of the surface area analyzer. Helium was used for the estimation of the dead volume, assuming that it is not adsorbed at any of the studied temperatures. To provide high accuracy and precision in determining P/P_0 , the saturation pressure P_0 was measured throughout the N₂ analyses by means of a dedicated saturation pressure transducer, which allowed us to monitor the vapor pressure for each data point. A part of the N₂ sorption isotherm in

the P/P_0 range 0.05-0.3 was fitted to the BET equation to estimate the BET surface area and the Langmuir surface area calculation was performed using all data points. The pore size distribution was obtained from the Horvath-Kawazoe (micropore) method in the Micromeritics ASAP2020 software package based on the N_2 sorption at 77K. The H_2 isotherm was measured at 77 K and the CO_2 and CH_4 isotherms were measured at 273 K.

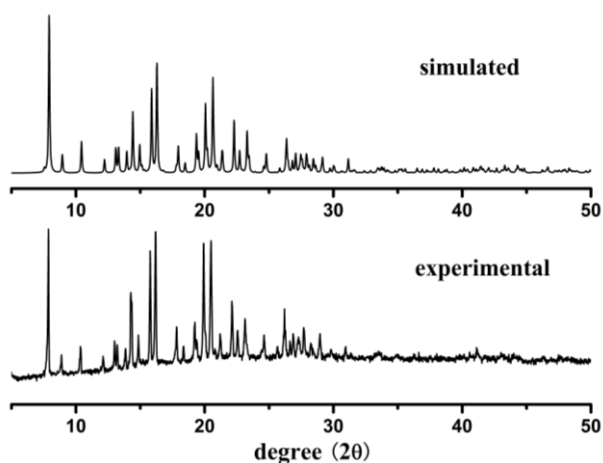


Fig. S1 Powder X-ray diffraction patterns of complex 1

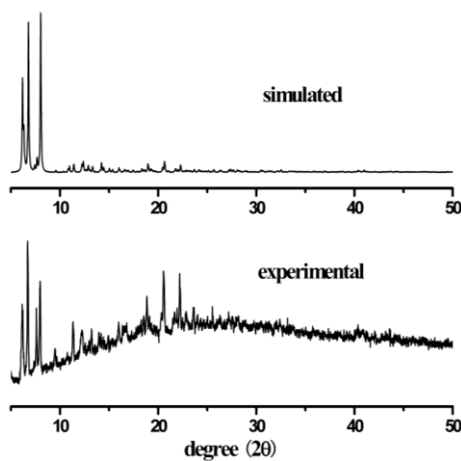


Fig. S2 Powder X-ray diffraction patterns of complex 2

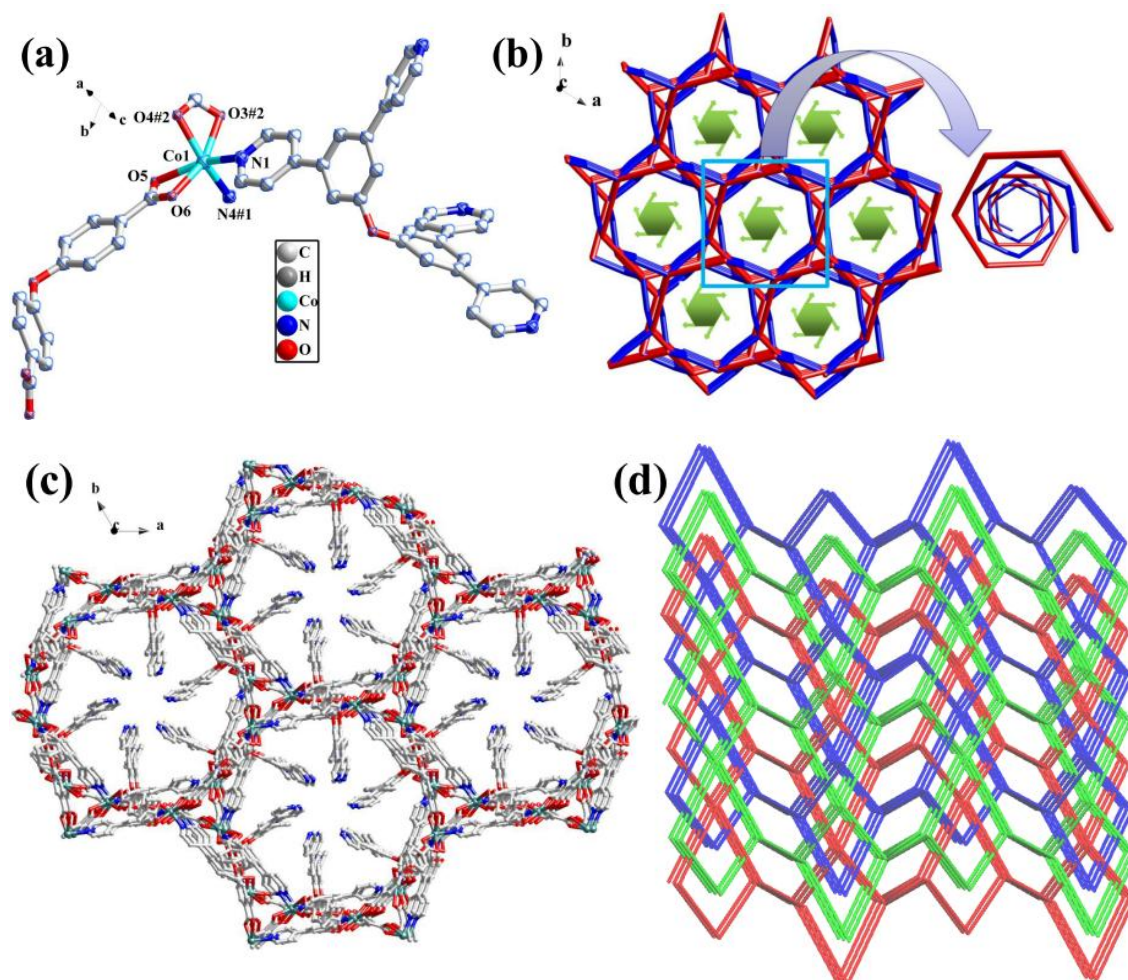


Fig. S3. (a) Coordination environment of **1** with 30% ellipsoid probability (hydrogen atoms and water molecules are omitted for clarity). Symmetry code: #1 = $x - y, x, -1/6 + z$. #2 = $1 + x - y, -1 + x, -1/6 + z$.; (b) A view of coaxial double-stranded helical chains possessing 6_5 screw axis along the *c* axis; (c) A perspective of 3D framework along the *c* axis with 1D helical channels occupied by the uncoordinated pyridyl groups of the L ligands (guest H₂O molecules are omitted); (d) Schematic representation of three fold interpenetrating framework with **qtz** topology.

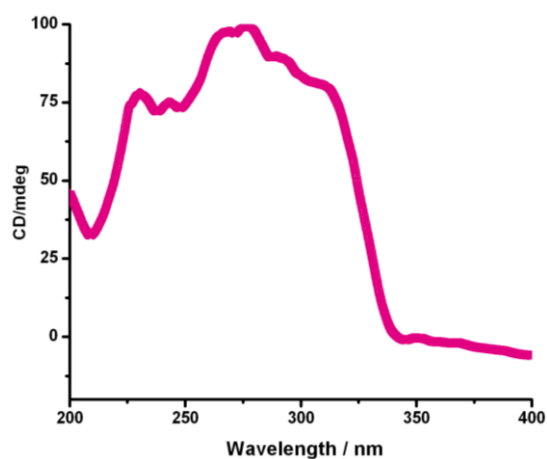


Fig. S4. The solid-state CD spectra of bulk samples of **1**.

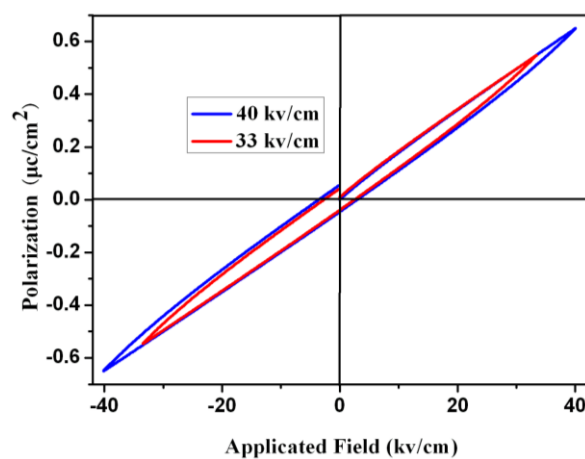


Fig. S5 An electric hysteresis loop of a pellet of powder of MOF **1** was observed by the virtual ground mode using a Precision Premier II ferroelectric tester at the temperature of liquid nitrogen.

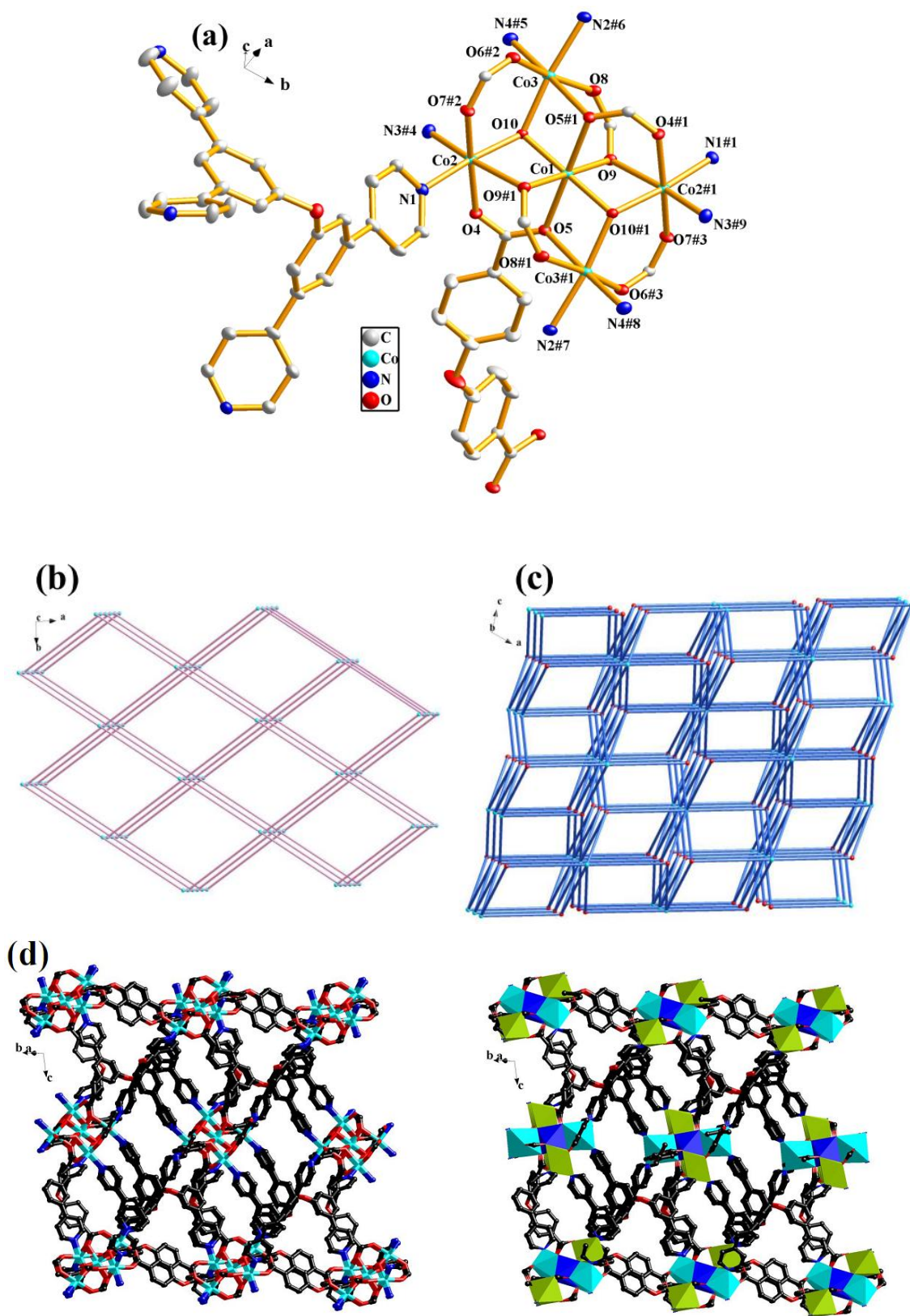


Fig. S6. (a) Coordination environment of 2 with 30% ellipsoid probability (hydrogen atoms and DMF molecules are omitted for clarity). Symmetry code: #1 = 2 - x, 2 - y, 2

- z; #2 = $1/2 + x, -1/2 + y, z$; #3 = $1/2 + x, -1/2 + y, z$; #4 = $x, 1 - y, 1/2 + z$; #5 = $2 - x, 1 - y, 2 - z$; #6 = $1/2 + x, 3/2 - y, 1/2 + z$; #7 = $3/2 - x, 1/2 + y, 3/2 - z$; #8 = $x, 1 + y, z$; #9 = $2 - x, 1 + y, 3/2 - z$. (b) A view of 3D **cds** formed by $[\text{Co}_5\text{O}_2]$ clusters and OBA ligands; (c) A view of 3D **alb** formed by $[\text{Co}_5\text{O}_2]$ clusters and L ligands; (d) Schematic representation of 3D framework of compound **2** without the guest DMF molecules, right: Co1 polyhedrons shown in blue, Co2 shown in turquoise, and Co3 shown in green.

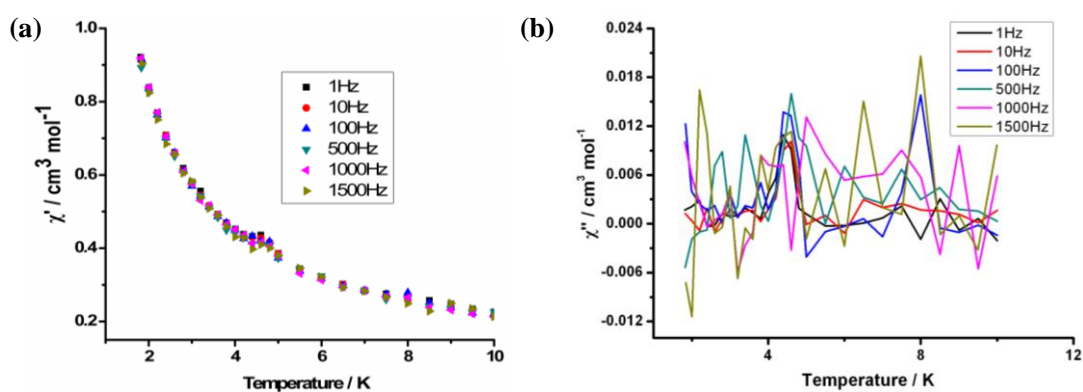


Fig. S7 Frequency dependence of the in-phase (a) and out-of-phase (b) ac susceptibility of **2** ($H_{\text{DC}} = 0$, $H_{\text{AC}} = 5$ G) at 1, 10, 100, 500, 1000, and 1500 Hz.

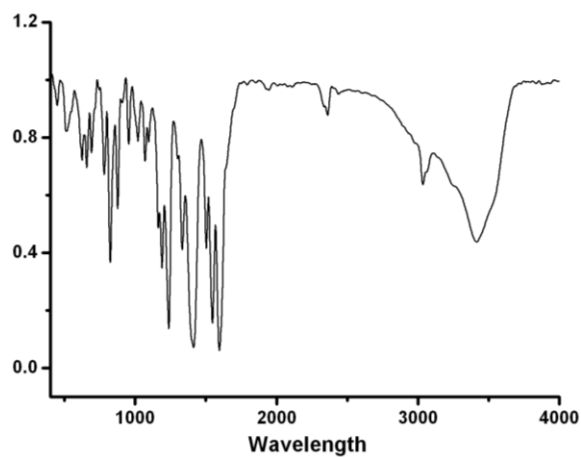


Fig. S8. IR spectra of complex **1**

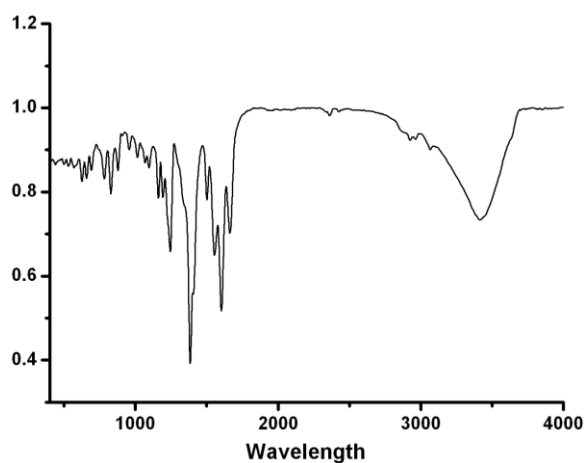


Fig. S9. IR spectra of complex **2**

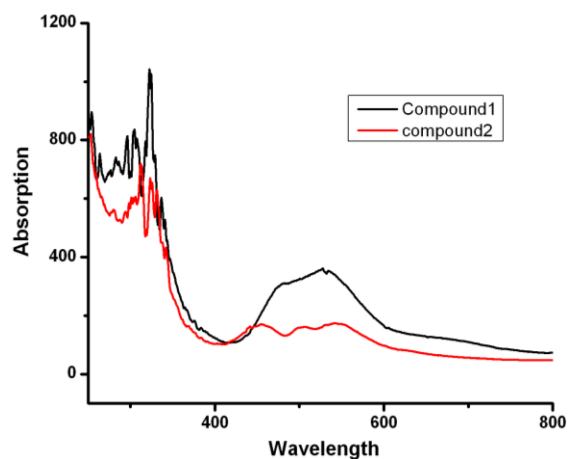


Fig. S10. UV-vis absorbance spectra of compounds **1** and **2** at room temperature.

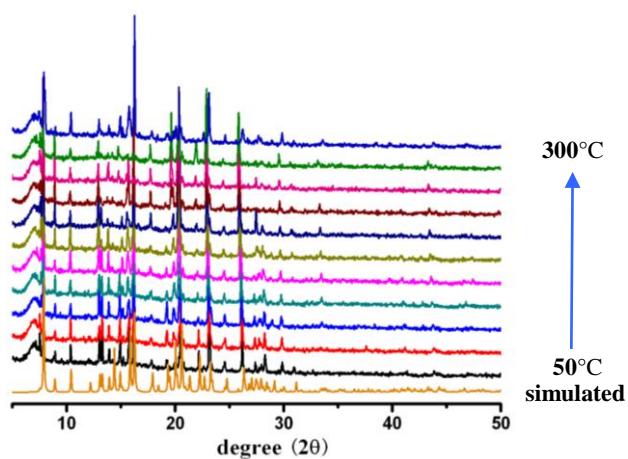


Fig. S11. VT-PXRD spectra of MOF **1** with heating (50-300 °C) showing thermal stability over a wide range of temperature.

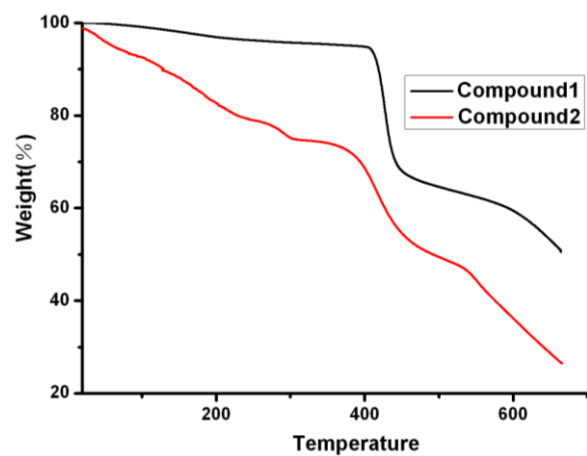


Fig. S12. The TGA diagrams of complexes **1** and **2**.

Table S1. Selected Bond Lengths (Å) and Angles (deg) for Complexes **1** and **2**

Complex 1			
Co1-N1	2.0728(16)	Co1-N4 ^a	2.0768(17)
Co1-O3 ^b	2.1852(15)	Co1-O4 ^b	2.1039(15)
Co1-O5	2.3203(14)	Co1-O6	2.0304(14)
N1-Co1-N4 ^a	98.20(6)	N1-Co1-O3 ^b	94.96(6)
N1-Co1-O4 ^b	99.60(6)	N1-Co1-O5	159.48(6)
N1-Co1-O6	99.13(6)	N4 ^a -Co1-O3 ^b	95.21(6)
N4 ^a -Co1-O4 ^b	151.48(6)	N4 ^a -Co1-O5	83.35(6)
N4 ^a -Co1-O6	97.94(6)	O3 ^b -Co1-O4 ^b	61.23(6)
O3 ^b -Co1-O5	105.31(5)	O3 ^b -Co1-O6	159.10(6)
O4 ^b -Co1-O5	87.64(6)	O4 ^b -Co1-O6	101
O5-Co1-O6	60.49(5)		
Complex 2			
Co1-O5	2.1650(14)	Co1-O5 ^a	2.1650(14)
Co1-O9	2.1218(14)	Co1-O9 ^a	2.1218(14)
Co1-O10	2.0237(14)	Co1-O10 ^a	2.0237(14)
Co2-O4	2.0541(14)	Co2-O7 ^b	2.0299(14)
Co2-O9 ^a	2.3151(15)	Co2-O10	2.0539(14)
Co2-N1	2.1293(17)	Co2-N3 ^c	2.1321(19)
Co3-O5 ^a	2.3374(15)	Co3-O6 ^b	2.0361(15)
Co3-O8	2.0689(15)	Co3-O10	2.0390(14)
Co3-N2 ^e	2.1640(19)	Co3-N4 ^d	2.169(2)
O5-Co1-O5 ^a	180	O5-Co1-O10 ^a	83.97(5)
O5-Co1-O9	91.29(5)	O5-Co1-O9 ^a	88.71(5)
O5-Co1-O10	96.03(6)	O5a-Co1-O10 ^a	96.03(6)

O5a-Co1-O9	88.71(5)	O5a-Co1-O9 ^a	91.29(5)
O5a-Co1-O10	83.97(5)	O9-Co1-O10 ^a	87.06(5)
O9-Co1-O9 ^a	180	O9-Co1-O10	92.94(5)
O9a-Co1-O10 ^a	92.94(5)	O9 ^a -Co1-O10	87.06(5)
O10 -Co1- O10 ^a	180	O4 - Co2- N3 ^c	90.84(7)
O4 - Co2- O7 ^b	172.55(6)	O4 - Co2- O9 ^a	86.58(5)
O4 - Co2- O10	89.26(6)	O4 - Co2- N1	89.14(6)
O7 ^b - Co2- N3 ^c	95.94(7)	O7 ^b - Co2- O9 ^a	87.15(6)
O7 ^b - Co2- O10	93.78(6)	O7 ^b - Co2- N1	87.11(6)
O9 ^a - Co2- N3 ^c	171.35(6)	O9 ^a - Co2- O10	87.15(6)
O9 ^a - Co2- N1	92.48(6)	O10 - Co2- N3 ^c	90.32(6)
O10- Co2- N1	173.75(6)	N1 - Co2- N3 ^c	95.74(7)
O5 ^a - Co3-N4 ^d	177.65(6)	O5 ^a - Co3-O6 ^b	91.69(18)
O5 ^a - Co3-O8	136.7(2)	O5 ^a - Co3-O10	79.37(5)
O5 ^a - Co3-N2 ^e	96.20(6)	O6 ^b - Co3- N4 ^d	92.89(7)
O6 ^b - Co3-O8	171.05(7)	O6 ^b - Co3-O10	98.04(6)
O6 ^b - Co3- N2 ^e	86.98(7)	O8 - Co3- N4 ^d	92.94(7)
O8 - Co3-O10	87.81(6)	O8 - Co3- N2 ^e	86.67(7)
O10 - Co3- N4 ^d	98.43(7)	O10 - Co3- N2 ^e	173.15(7)
N2 ^e - Co3- N4 ^d	85.91(8)		

Symmetry Codes: for **1**: a = $x - y, x, -1/6 + z$; b = $1 + x - y, -1 + x, -1/6 + z$. for **2**: a = $2 - x, 2 - y, 2 - z$; b = $1/2 + x, -1/2 + y, z$; c = $x, 1 - y, 1/2 + z$; d = $2 - x, 1 - y, 2 - z$; e = $1/2 + x, 3/2 - y, 1/2 + z$.

References

1. M. A. Alam, A. Tsuda, Y. Sei, K. Yamaguchi and T. Aida, *Tetrahedron* 2008, **64**, 8264.
2. *SAINT*, Version 6.02a; Bruker AXS Inc.: Madison, WI, 2002.
3. G. M. Sheldrick, *SADABS, Program for Bruker Area Detector Absorption*

Correction, University of Göttingen, Göttingen, Germany, 1997.

4. Platon Program: A. L. Spek, *Acta Cryst. Sect. A*. 1990, **46**, 194.